An Evaluation of Wireless Power Transfer System with Plural Repeater Coils for Moving Objects

Tatsuya Yamamoto
Graduate school of Science and Engineering
Saitama University
Saitama, Japan
Email: grgrstar@gmail.com

Kenji Nara
Graduate school of Science and Engineering.
Saitama University
Saitama, Japan
Email: k.nara.495@ms.saitama-u.ac.jp

Yasuyoshi Kaneko
Graduate school of Science and Engineering.
Saitama University
Saitama, Japan
Email: kaneko@ees.saitama-u.ac.jp

***Abstract*— In this paper, we study the use of Wireless Power Transfer (WPT) for feeding Electric Vehicles (EV) and other conveyance machines. We researched circuit topologies that can be extended to a bidirectional feed and are suitable as feeds for moving objects, and proposed two systems; a two-repeater coils system and a Parallel-Parallel compensation capacitor system (PP system), which are symmetrical circuit configurations on the primary and secondary side transfer. The results show that the immittance converter characteristics can be obtained by optimal design of the capacitor. Based on the power feeding experimental result, it was confirmed that the input power can be suppressed by increasing the input impedance at the time of shifting the position of the secondary side. We demonstrate the usefulness of the two-repeater coils system and PP system, assuming the use of multiple ground coils.**

Keywords—Wireless power transfer, Repeater coil, Plural repeater coils, Compensation capacitor

I. INTRODUCTION

Recently, Plug-in Hybrid Vehicles (PHVs) and Electric Vehicles (EVs) are being promoted as new vehicles replacing those powered by gasoline due to considerations of global environmental problems and effective use of energy. A conductive type of connection using electric cables and connectors is used for charging EVs at present. However, with this method, there are the problems that wear can occur when attaching and detaching the connector, or that spontaneous electric shocks can occur if it is raining. It is therefore expected that establishing a charging method based on Wireless Power Transfer (WPT) [1] will be superior to the conductive method in terms of convenience, safety, and maintainability through cordless technology. WPT is adopted not only for EVs but also for equipment used in factories. For cleanrooms and buildings which require painting work, WPT is utilized for charging and driving Automated Guided Vehicles (AGVs) and conveyance machines used for transporting parts and the like.

For supplying power to the functional EV, multiple coils are arranged on the ground side [2] that are switched on to be energized depending on the presence or absence of the vehicle. Using a one-repeater coil system, which has a third coil between the primary and secondary coil, or a Parallel-Series compensation capacitor (PS) system, which has a compensation capacitor in parallel on the primary side and in series on the secondary side, there is a possibility that the ground side coils connected in parallel can be switched without a control mechanism when driving at constant voltage [3]. However, in these systems, it is necessary to increase the number of turns of the coil on the secondary side with respect to that on the primary side, which may be difficult to design. Furthermore, because the circuit configuration is asymmetrical between the primary and secondary side, it is difficult to extend to bidirectional feeding [4].

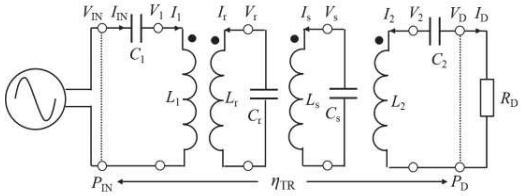

Fig. 1 Circuit of Two-Repeater Coils WPT System

Research on the practical application of bidirectional power supply to allow electrical power to be interchanged for houses is also being conducted, as is research for EVs incorporating their own mobile battery. When the battery capacity decreases, it is charged to the EV from the house or electric power system, whereas on the contrary, electricity is supplied to the house in the case of emergency when the power system is down. In addition, to return the power to the power supply side by regenerative braking with WPT while the conveyor is moving, a mechanism such as bidirectional feeding is required.

Therefore, in this research, we propose a design guideline by systematically summarizing characteristics of circuit topology which can be extended to bidirectional feed and is suitable for a feed to moving objects. We perform a theoretical analysis of the two-repeater coils system, in which the repeater coil is wound in close contact with the coils of both the primary and secondary side, and the Parallel-Parallel compensation capacitor (PP) system [5], which is considered to have characteristics similar to the two-repeater coils system. The validity of the theoretical equation is verified by a power feeding experiment using real equipment.

II. TWO-REPEATER COILS WPT SYSTEM

A. Circuit of Two-Repeater Coils WPT System

The circuit configuration of the two-repeater coils system is shown in Fig. 1. In this system, there are two windings of the repeater coil between the primary and secondary side, and

compensation capacitors are connected in series to all coils. Subsequently, the winding (coil) resistance and iron loss are assumed to be sufficiently smaller than the impedance of the coil at high frequencies. The relationship between the voltage and the current of each coil is represented by (1) using the impedance matrix.

$$\begin{pmatrix} V_{IN} \\ 0 \\ 0 \\ 0 \end{pmatrix} = \begin{pmatrix} j\omega L_1 + \frac{1}{j\omega C_1} & j\omega M_{12} & j\omega M_{1r} & j\omega M_{1s} \\ j\omega M_{12} & j\omega L_2 + \frac{1}{j\omega C_2} + R_D & j\omega M_{2r} & j\omega M_{2s} \\ j\omega M_{1r} & j\omega M_{2r} & j\omega L_r + \frac{1}{j\omega C_r} & j\omega M_{rs} \\ j\omega M_{1s} & j\omega M_{2s} & j\omega M_{rs} & j\omega L_s + \frac{1}{j\omega C_s} \end{pmatrix} \begin{pmatrix} I_1 \\ I_2 \\ I_r \\ I_s \end{pmatrix} \quad (1)$$

These values are the voltage V, current I, compensation capacitance C, self-inductance L, as shown in Fig.1, mutual inductance M_{ij} (i,j = 1,2,r,s) between the primary and secondary coil and repeater coils (r coil and s coil, respectively), and angular frequency ω (= $2\pi f_0$) of the power supply.

First, the capacitor values are determined as shown in (2), so as to resonate with the self-inductance of the repeater coil as in the conventional one-repeater coil system.

$$C_r = \frac{1}{\omega^2 L_r}, \quad C_s = \frac{1}{\omega^2 L_s} \quad (2)$$

From (1) and (2), it is possible to obtain the immittance converter characteristics and set the input power factor to 1 by setting the values of the primary and secondary side capacitor as shown in (3).

$$C_1 = \frac{1}{\omega^2 L_1\left(1 - \frac{2k_{1r}k_{1s}}{k_{rs}}\right)}, \quad C_2 = \frac{1}{\omega^2 L_2\left(1 - \frac{2k_{2r}k_{2s}}{k_{rs}}\right)} \quad (3)$$

Here, k_{ij} (i,j = 1,2,r,s) is the coupling coefficient between the coils.

In real situations, when winding the two repeater coils in close contact with the primary and secondary side coil, the following problem arises with this method of determining capacitance. Assuming that the primary side and r coil and the secondary side and s coil are tightly coupled, the coupling coefficient is expressed by (4).

$$k_{1r} = k_{2s} = 1 \quad (4)$$

In addition, it is assumed that all other coupling coefficients between the coils are equal to k.

$$k_{12} = k_{rs} = k_{1s} = k_{2r} = k \quad (5)$$

In this situation, the primary and secondary side capacitances are represented by the expressions show in (6), which take a negative value. This causes problems for practical use.

$$C_1 = \frac{1}{\omega^2(-L_1)}, \quad C_2 = \frac{1}{\omega^2(-L_2)} \quad (6)$$

B. Circuit Characteristics during Capacitor Correction

In order to prevent the primary and secondary capacitors from taking a negative value, it suffices that the denominator of the capacitance formula becomes 0 when they come into close contact with the repeater coil. We therefore modify it, as shown in (7), and proceed with the analysis based on this.

$$C_1 = \frac{1}{\omega^2 L_1\left(1 - \frac{k_{1r}k_{1s}}{k_{rs}}\right)}, \quad C_2 = \frac{1}{\omega^2 L_2\left(1 - \frac{k_{2r}k_{2s}}{k_{rs}}\right)} \quad (7)$$

From (1) and (7), the compensation capacitor value of the repeater section with input/output power characteristics matching the immittance converter characteristics and an input power factor that becomes 1 is as follows.

$$C_r = \frac{1}{\omega^2 L_r\left(1 - \frac{k_{2r}k_{rs}}{k_{2s}}\right)}, \quad C_s = \frac{1}{\omega^2 L_s\left(1 - \frac{k_{1s}k_{rs}}{k_{1r}}\right)} \quad (8)$$

The input/output characteristics are expressed by (9).

$$\begin{pmatrix} V_{IN} \\ I_{IN} \end{pmatrix} = \begin{pmatrix} 0 & j\omega\frac{k_{1r}k_{2s} - k_{12}k_{rs}}{k_{rs}}\sqrt{L_1L_2} \\ -\frac{1}{j\omega}\frac{k_{rs}}{k_{1r}k_{2s} - k_{12}k_{rs}}\frac{1}{\sqrt{L_1L_2}} & 0 \end{pmatrix} \begin{pmatrix} V_D \\ I_D \end{pmatrix} \quad (9)$$

From (9), the self-inductance (and the number of turns) of the two-repeater coils is irrelevant to the input/output characteristics of the WPT circuit. The input impedance Z_{IN} is then obtained as shown in (10).

$$Z_{IN} = \left(\omega\frac{k_{1r}k_{2s} - k_{12}k_{rs}}{k_{rs}}\right)^2 L_1L_2\frac{1}{R_D} \quad (10)$$

Here, when the coupling coefficient satisfies the conditions of (4) and (5), (10) can be rewritten as (11).

$$Z_{IN} = \left\{\omega\left(\frac{1}{k} - k\right)\right\}^2 L_1L_2\frac{1}{R_D} \quad (11)$$

Equation (11) shows that the input impedance increases as the coupling coefficient decreases (such that the position shift increases), and that the input current can be suppressed when driving with constant input voltage.

Next, ignoring the iron loss, the transformer efficiency is given by following (12).

$$\begin{aligned} \eta_{TR} &= \frac{R_D}{\frac{r_1M_{rs}^2 + r_sM_{1r}^2}{\omega^2(M_{1r}M_{2s} - M_{12}M_{rs})^2}R_D^2 + R_D + r_2 + r_r\left(\frac{M_{2s}}{M_{rs}}\right)^2} \\ &= \frac{R_D}{\frac{k_{rs}^2Q_s + k_{1r}^2Q_1}{r_2Q_1Q_2Q_s(k_{1r}k_{2s} - k_{12}k_{rs})^2}R_D^2 + R_D + r_2\left(1 + \frac{k_{2s}^2Q_2}{k_{rs}^2Q_r}\right)} \end{aligned} \quad (12)$$

Q (= $\omega L/r$) is an index representing the performance of the coil. For $\partial\eta_{TR}/\partial R_D = 0$, the maximum efficiency $\eta_{TR\max}$ and the load resistance value $R_{D\max}$ at the maximum efficiency (optimum load) are obtained as follows.

$$R_{D\max} = \frac{k_{1r}k_{2s} - k_{12}k_{rs}}{k_{rs}} r_2 Q_2 \sqrt{\frac{k_{rs}^2 Q_r + k_{2s}^2 Q_2}{k_{rs}^2 Q_s + k_{1r}^2 Q_1} \frac{Q_1 Q_s}{Q_2 Q_r}}$$

$$\eta_{TR\max} = \frac{1}{1 + \frac{2}{(k_{1r}k_{2s} - k_{12}k_{rs})k_{rs}Q_rQ_s} \sqrt{\left(k_{rs}^2 Q_r + k_{2s}^2 Q_2\right)\left(k_{rs}^2 Q_s + k_{1r}^2 Q_1\right)\frac{Q_r Q_s}{Q_1 Q_2}}} \quad (13)$$

C. Comparison with Magnetic Resonant Coupling System

A magnetic resonant coupling system [6] proposed by MIT is cited as a WPT method with four coils from the power supply to the load configured like the two-repeater coils system. Fig. 2 shows a diagram of WPT by the magnetic resonant coupling system. It is said that the magnetic resonant coupling system is equivalent to the SS system in terms of its electric circuit [7] [8]. In this section, based on the description in section II-*B*, we show that both methods are equivalent in their mathematical equations with regards to the input/output characteristics and power supply efficiency.

When mutual coupling exists only between adjacent coils (primary side and *r* coil, *r* and *s* coil, *s* and secondary side coil), the coupling coefficients other than k_{1r}, k_{rs}, and k_{2s} are all 0. In this case, the capacitor values take the form shown in (14), and it is found that they are determined the values to resonance with each associated self-inductance value.

$$C_1 = \frac{1}{\omega^2 L_1},\ C_2 = \frac{1}{\omega^2 L_2},\ C_r = \frac{1}{\omega^2 L_r},\ C_s = \frac{1}{\omega^2 L_s} \quad (14)$$

The input/output characteristics are expressed by (15), and when $\tilde{M} = \frac{M_{rs}}{M_{1r}M_{2s}}$, $\tilde{k} = \frac{k_{rs}}{k_{1r}k_{2s}}$, the equation is rewritten as (16).

$$\begin{pmatrix} V_{IN} \\ I_{IN} \end{pmatrix} = \begin{pmatrix} 0 & j\omega \frac{k_{1r}k_{2s}}{k_{rs}} \sqrt{L_1 L_2} \\ -\frac{1}{j\omega} \frac{k_{rs}}{k_{1r}k_{2s}} \frac{1}{\sqrt{L_1 L_2}} & 0 \end{pmatrix} \begin{pmatrix} V_D \\ I_D \end{pmatrix} \quad (15)$$

$$\begin{pmatrix} V_{IN} \\ I_{IN} \end{pmatrix} = \begin{pmatrix} 0 & j\omega\tilde{M} \\ -\frac{1}{j\omega\tilde{M}} & 0 \end{pmatrix} \begin{pmatrix} V_D \\ I_D \end{pmatrix} = \begin{pmatrix} 0 & j\omega\tilde{k}\sqrt{L_1 L_2} \\ -\frac{1}{j\omega\tilde{k}} \frac{1}{\sqrt{L_1 L_2}} & 0 \end{pmatrix} \begin{pmatrix} V_D \\ I_D \end{pmatrix} \quad (16)$$

Power supply efficiency is given by (17), and when $\tilde{r}_1 = r_1 + r_s\left(\frac{M_{1r}}{M_{rs}}\right)^2$, $\tilde{r}_2 = r_2 + r_r\left(\frac{M_{2s}}{M_{rs}}\right)^2$, the equation is rewritten as (18).

$$\eta_{TR} = \frac{R_D}{\frac{r_1 + r_s\left(\frac{M_{1r}}{M_{rs}}\right)^2}{\left(\omega\frac{M_{1r}M_{2s}}{M_{rs}}\right)^2} R_D^2 + R_D + r_2 + r_r\left(\frac{M_{2s}}{M_{rs}}\right)^2} \quad (17)$$

$$\eta_{TR} = \frac{R_D}{\frac{\tilde{r}_1}{\left(\omega\tilde{M}\right)^2} R_D^2 + R_D + \tilde{r}_2} \quad (18)$$

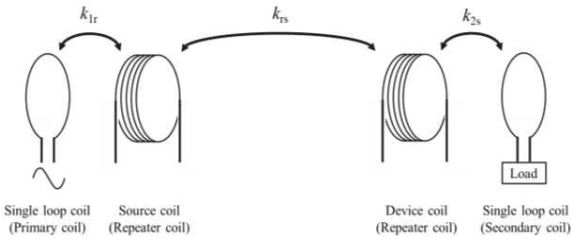

Fig. 2 Pattern Diagram of WPT by Magnetic Resonant Coupling System

Table I. Comparison between Magnetic Resonant Coupling and SS method

	Magnetic Resonant Coupling	SS
C	$C_1 = \frac{1}{\omega^2 L_1}, C_2 = \frac{1}{\omega^2 L_2}$ $C_r = \frac{1}{\omega^2 L_r}, C_s = \frac{1}{\omega^2 L_s}$	$C_1 = \frac{1}{\omega^2 L_1}, C_2 = \frac{1}{\omega^2 L_2}$
Input / Output char	$\begin{cases} V_{IN} = j\omega\tilde{k}\sqrt{L_1 L_2} I_D \\ I_{IN} = -\frac{1}{j\omega\tilde{k}} \frac{1}{\sqrt{L_1 L_2}} V_D \end{cases}$	$\begin{cases} V_{IN} = -j\omega k\sqrt{L_1 L_2} I_D \\ I_{IN} = \frac{1}{j\omega k} \frac{1}{\sqrt{L_1 L_2}} V_D \end{cases}$
Z_{IN}	$Z_{IN} = \left(\omega\tilde{M}\right)^2 \frac{1}{R_D}$	$Z_{IN} = \left(\omega M\right)^2 \frac{1}{R_D}$
η_{TR}	$\eta_{TR} = \frac{R_D}{\frac{1}{\tilde{k}^2 \tilde{r}_2 \tilde{Q}_1 \tilde{Q}_2} R_D^2 + R_D + \tilde{r}_2}$	$\eta_{TR} = \frac{R_D}{\frac{1}{k^2 r_2 Q_1 Q_2} R_D^2 + R_D + r_2}$
$R_{D\max}$	$R_{D\max} = \tilde{k}\tilde{r}_2\sqrt{\tilde{Q}_1\tilde{Q}_2}$	$R_{D\max} = k r_2 \sqrt{Q_1 Q_2}$
$\eta_{TR\max}$	$\eta_{TR\max} = \frac{1}{1 + \frac{2}{\tilde{k}\sqrt{\tilde{Q}_1\tilde{Q}_2}}}$	$\eta_{TR\max} = \frac{1}{1 + \frac{2}{k\sqrt{Q_1 Q_2}}}$

From this, the optimum load $R_{D\max}$ and the maximum efficiency $\eta_{TR\max}$ are obtained as shown in (19) with $\tilde{Q}_1 = \frac{\omega L_1}{\tilde{r}_1}$, $\tilde{Q}_2 = \frac{\omega L_2}{\tilde{r}_2}$.

$$R_{D\max} = \omega\tilde{M}\sqrt{\frac{\tilde{r}_2}{\tilde{r}_1}} = \tilde{k}\tilde{r}_2\sqrt{\tilde{Q}_1\tilde{Q}_2}$$
$$\eta_{TR\max} = \frac{1}{1 + \frac{2}{\omega\tilde{M}}\sqrt{\tilde{r}_1\tilde{r}_2}} = \frac{1}{1 + \frac{2}{\tilde{k}\sqrt{\tilde{Q}_1\tilde{Q}_2}}} \quad (19)$$

Table I compares the respective values of the magnetic resonant coupling system and the SS system [9]. Although the positive and negative signs of the input/output characteristics are reversed, it can be confirmed that the circuit characteristics in the two schemes. From the above, it can be seen that the magnetic resonant coupling system is also equivalent to the SS system with respect to the mathematical description, except that the sign of the input/output characteristics differs.

III. Parallel-Parallel WPT System

A. Circuit of Parallel-Parallel WPT System

The circuit configuration of the PP system is shown in Fig. 3. In the PP system, capacitors are connected in parallel to the coils on both the primary and secondary sides. Because there is only one mutual coupling, and because it can be regarded as a transformer with a gap, it is represented by the T-type equivalent circuit shown in Fig. 4. We calculate the F-matrix of the T-type equivalent circuit and obtain the capacitor values such that its diagonal component is 0 as shown in (20). Unlike the conventional design method [10], it is determined independently of the load resistance.

$$C_1 = \frac{1}{\omega^2 L_1\left(1-k^2\right)},\ C_2 = \frac{1}{\omega^2 L_2\left(1-k^2\right)} \tag{20}$$

The input/output characteristics are obtained by substituting (20) into the F-matrix and are expressed by (21).

$$\begin{pmatrix} V_{IN} \\ I_{IN} \end{pmatrix} = \begin{pmatrix} 0 & j\omega\dfrac{1-k^2}{k}\sqrt{L_1L_2} \\ -\dfrac{1}{j\omega}\dfrac{k}{1-k^2}\dfrac{1}{\sqrt{L_1L_2}} & 0 \end{pmatrix} \begin{pmatrix} V_D \\ I_D \end{pmatrix} \tag{21}$$

As for the two-repeater coils system, the immittance converter characteristics are obtained and the input power factor is also 1. The input impedance is given by (22), which shows that it increases as the coupling coefficient decreases (corresponding to increasing position shift).

$$Z_{IN} = \left\{\omega\left(\frac{1}{k}-k\right)\right\}^2 L_1L_2\frac{1}{R_D} \tag{22}$$

The transformer efficiency (ignoring iron loss) is calculated and expressed by (23), and the optimum load $R_{D\max}$ and the maximum efficiency $\eta_{TR\max}$ are obtained as shown in (24).

$$\begin{aligned} \eta_{TR} &= \frac{R_D}{\dfrac{r_1M^2+r_2L_1^2}{\omega^2\left(L_1L_2-M^2\right)^2}R_D^{\,2}+R_D+r_2+r_1\left(\dfrac{L_2}{M}\right)^2} \\ &= \frac{R_D}{\dfrac{1}{r_2Q_2^{\,2}}\dfrac{1}{\left(1-k^2\right)^2}\dfrac{k^2Q_2+Q_1}{Q_1}R_D^{\,2}+R_D+r_2\dfrac{k^2Q_1+Q_2}{k^2Q_1}} \end{aligned} \tag{23}$$

$$\begin{aligned} R_{D\max} &= \frac{1-k^2}{k}r_2Q_2\sqrt{\frac{k^2Q_1+Q_2}{k^2Q_2+Q_1}} \\ \eta_{TR\max} &= \frac{1}{1+\dfrac{2}{\left(1-k^2\right)kQ_1Q_2}\sqrt{\left(k^2Q_1+Q_2\right)\left(k^2Q_2+Q_1\right)}} \end{aligned} \tag{24}$$

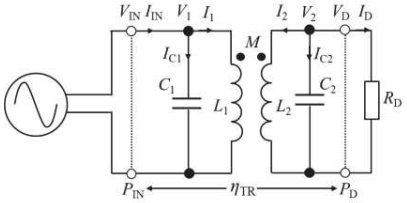

Fig. 3 Circuit of Parallel-Parallel WPT System

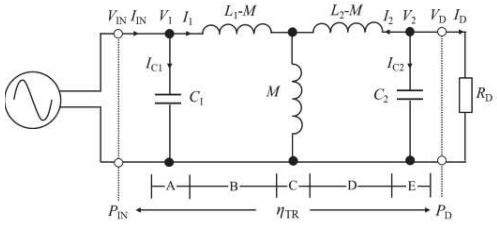

Fig. 4 T-type Equivalent Circuit of PP System

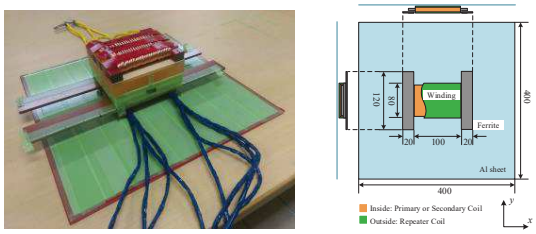

(a) Appearance (b) Dimensions

Fig. 5 Transformer Used in the Experiment

B. Comparison between PP and Two-Repeater Coils System

In the two-repeater coils system, as described above, when two repeater coils are wound in close contact with the primary and secondary side coil (in consideration of the real situation), it is assumed that the coupling coefficient satisfies the conditions of (4) and (5). We also consider using coils with the same performance (equal Q values). Under this condition, the primary and secondary capacitances $C_1 \to \infty$, $C_2 \to \infty$ (and reactance is 0) according to (7). In addition, the capacitance of the repeater section is given by (25), and has the same form as (20) which determines the capacitor values of the PP system.

$$C_r = \frac{1}{\omega^2 L_r\left(1-k^2\right)},\ C_s = \frac{1}{\omega^2 L_s\left(1-k^2\right)} \tag{25}$$

Furthermore, calculation of the input/output characteristics, input impedance, and power supply efficiency is also analogous to (21) to (24) in the PP system. From these observations, it was found that the two-repeater coils system is equivalent to the PP system depending on how the repeater coils are wound.

IV. Power Feeding Experiment of the Two Systems

In order to verify whether the results of the two-repeater coils system and the PP system from theoretical analysis can also be realized in an actual machine, we fabricated transformers and measured constants corresponding to both methods. The appearance and dimensions of the transformer used are shown in Fig. 5. The coil shape was solenoidal. In the

Table II. Transformer Parameter

Topology	Two-Repeater Coils	PP
Gap length [mm]	60.0	
N_1 [Turn]	4	4
N_r [Turn]	18	-
N_s [Turn]	18	-
N_2 [Turn]	4	4
r_1 [mΩ]	9.79	12.8
r_r [mΩ]	105	-
r_s [mΩ]	105	-
r_2 [mΩ]	10.5	11.6
L_1 [μH]	6.78	5.83
L_r [μH]	54.0	-
L_s [μH]	55.5	-
L_2 [μH]	6.71	6.03
k_{12}	0.201	0.226
k_{rs}	0.245	-
k_{1s}	0.237	-
k_{2r}	0.229	-
k_{1r}	0.924	-
k_{2s}	0.930	-
$\|Z_{in}\|$ [Ω]	11.8	12.3
R_{Dmax} [Ω]	12.1	14.4
η_{TRmax} [%]	96.8	96.4

two-repeater coils system, repeater coils were wound so as to be closely contacted from above the coils of the primary and secondary side. In order to reduce the current flowing through the repeater coil, the number of turns was set to 4.5 times the number of turns of the primary and secondary side coil. In addition, in order to prevent excessive voltage [11], the split capacitor method was adopted with the coil divided into 2 for every 9 turns. Aluminum plates were installed on the back of the primary and secondary coils for both methods. Table II shows the measured results when the gap of the transformers is 60 mm and in the standard state without position shift. In the two-repeater coils system, k_{1r} and k_{2s} were 0.9 or greater, which means that there was stronger coupling than for the other coils.

We conducted power feeding experiments of the two-repeater coils system and the PP system using the specifically-fabricated transformers. Table III displays the conditions during power supply and Fig. 6 shows the experimental circuit. A square wave inverter was used as the power supply. In order to confirm the characteristics at the fundamental frequency f_0 = 85.0 kHz, a band pass filter was inserted into the power output section with a sine wave input. The load resistance R_L after the rectification was set to a value at which the transformer efficiency η_{TR} was maximized. The DC input voltage V_{DC} was adjusted so that the output power P_L after the rectification reached 1.5 kW in the standard state for each method.

Input waveforms at the time of power supply in the standard state are shown in Fig. 7. The voltage and current waveforms of both methods were almost identical. Also, due to capacitor compensation, the input power factor was almost 1 in

Table III. Experimental Conditions

Topology	Two-Repeater Coils	PP
f_0 [kHz]	85.0	
R_L [Ω]	25.0	30.0
C_1 [μH]	4.90	0.587
C_r [μH]	0.0629	-
C_s [μH]	0.0696	-
C_2 [μH]	4.34	0.629
L_f [μH]	104	
C_f [μF]	0.0336	

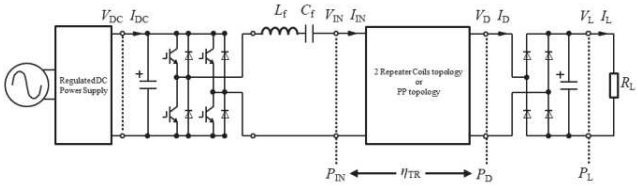

Fig. 6 Experimental Circuit

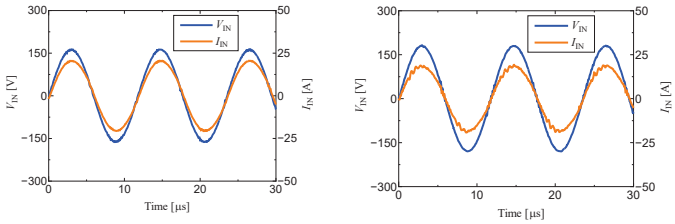

(a) Two-Repeater Coils System (b) PP System

Fig. 7 Input Waveforms in Standard State

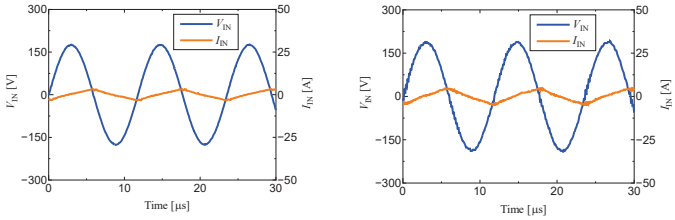

(a) Two-Repeater Coils System (b) PP System

Fig. 8 Input Waveforms Secondary Side Absence

both cases. Comparing the circulating currents, in the PP system I_1 = 41.3 A and I_2 = 53.8 A, which are larger than the input/output currents (I_{IN} = 13.1 A, I_D = 12.9 A), but in the two-repeater coils system, I_r = 12.1 A and I_s = 18.8 A, which is about a third of the PP system currents. It was confirmed that the circulating current could be drastically reduced using a repeater coil with many more turns than the primary and secondary side coils. In addition, by using the split capacitor method, the voltage across the terminals of the coil reached a maximum of 255 V, which was only 1.5 times as much as the highest alternating voltage V_D = 165 V in the PP system.

In the case of secondary side absence, input waveforms are shown in Fig. 8. By comparing these results with those of the

standard state shown in Fig. 7, it was confirmed that the peak value of the input current I_{IN} and the input power factor were greatly reduced in both systems. Variations of the input impedance | Z_{IN} | and the input power P_{IN} in the case of misalignment are shown in Fig. 9 and 10. We confirmed that | Z_{IN} | increases and P_{IN} decreases in the case of misalignment in both systems when V_{DC} is constant.

V. Conclusion

In this research, we studied two types of circuit topologies that can suppress the input power for the case of secondary side misalignment or absence when driven with constant input voltage. We conducted a circuit analysis of the two-repeater coils system, in which a repeater coil was added to each of two windings to make a transmitting and receiving coil. We analyzed the case where capacitor compensation was carried out by the same determination method as for the conventional one-repeater coil system and outlined an immediate practical problem that arises. In order to solve this problem, the method of capacitor compensation was modified to obtain adequate circuit characteristics, power supply efficiency, etc. Furthermore, applying the condition of no coupling between non-adjacent coils, we analyzed the magnetic resonance coupling system using four coils as in the two-repeater coils system and proved that it is equivalent to the SS system.

Next, we conducted a circuit analysis on the PP system, which is considered to have characteristics similar to the two-repeater coils system. Comparing the two systems, the input/output characteristics and the power supply efficiency were similar, depending on the conditions.

We also verified the validity of the theory behind the two-repeater coils and PP systems through a power supply experiment using real equipment. It was confirmed that the input power is reduced by changing the input impedance and the input power factor in the case of secondary side misalignment or absence.

As described above, the two-repeater coils and PP systems, which have symmetrical circuit configurations on the primary and secondary side, exhibit immittance converter characteristics useful for batteries that require charging with a constant current. This, and the findings that the input power can be suppressed in the case of secondary side misalignment are useful characteristics for power supplies of moving objects, and we have shown the usefulness of the method proposed here.

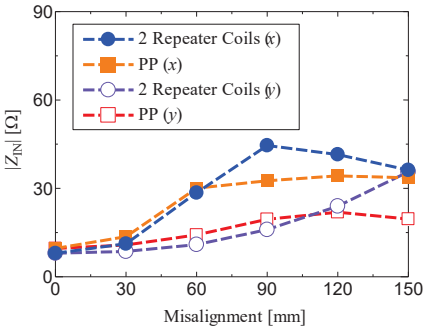

Fig.9 $|Z_{IN}|$ in Secondary Side Misalignment

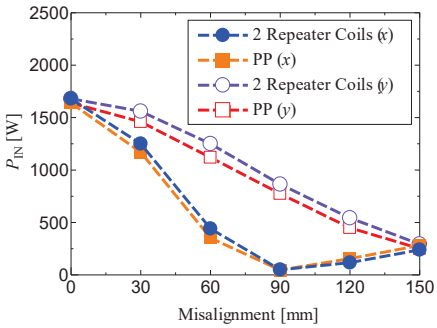

Fig.10 P_{IN} in Secondary Side Misalignment

References

[1] G. A. Covic and J. T. Boys, "Modern trends in inductive power transfer for transportation application", IEEE J. Emerg. Sel. Topics Power Electron., vol. 1, no. 1, pp. 28–41, 2013.

[2] J. M. Miller, P.T. Jones, J-M. Li, and O. C. Onar, "ORNL Experience and Challenges Facing Dynamic Wireless Power Charging of EV's", IEEE Circuits and Systems Magazine, pp. 40-53, 2015.

[3] J. Yamada, K. Tsuda, R. Kobayashi, and Y. Kaneko, "Circuit Analysis and Characterization of Contactless Power Transfer System with Variable Impedance", IEEJ Transactions on Industry Applications, vol. 137, no. 11, pp. 815-826, 2017.

[4] S. Nakadachi, S. Mochizuki, S. Sakaino, Y. Kaneko, S. Abe, and T. Yasuda, "Bidirectional Contactless Power Transfer System Expandable from Unidirectional System", ECCE2013, Denver, P505, 2013.

[5] T. Yamamoto and Y. Kaneko, "An Evaluation of Wireless Power Transfer System with Plural Repeater Coils for Moving Objects", IEEJ, 2018.

[6] A. Kurs, A. Karalis, R. Moffatt, J. D. Joannopoulos, P. Fisher, and M. Soljacic, "Wireless Power Transfer via Strongly Coupled Magnetic Resonances", Science Express on 7 June 2007, vol. 317, no. 5834, pp. 83-86, 2007.

[7] N. Hagiwara, "Study on the Principle of Contactless Electric Power Transfer via Electromagnetic Coupling", IEEJ Transactions on Industry Applications, vol. 131, issue. 5, pp. 708-713, 2011.

[8] T. Imura and Y. Hori, "Unified theory of electromagnetic and magnetic resonant coupling", IEEE Transactions on Industry Applications, vol. 135, no. 6, pp. 697-710, 2015.

[9] T. Tohi, Y. Kaneko, and S. Abe, "Maximum Efficiency of Contactless Power Transfer Systems using k and Q", IEEJ The papers of Technical Meeting on SPC-11-179, 2011.

[10] Chewi-Sen Wang, O. H. Stielau, and G. A. Covic, "Design Considerations for a Contactless Electric Vehicle Battery Charger", IEEE TRANSACTIONS ON INDUSTRIAL ELECTRONICS, vol. 52, no. 5, pp. 1308-1324, 2005.

[11] T. Yamamoto and Y. Kaneko, "A Study of the Common Use of Wireless Power Transfer System Which Has a Difference in the Magnetic Field Structure", IEEJ Transactions on Industry Applications, 1-94, pp. 327-332, 2015.